Mon. Not. R. Astron. Soc. **322**, 933–944 (2001)

The Second APM UKST Colour Survey for $z > 4$ quasars

Lisa J. Storrie-Lombardi,[1★] Michael J. Irwin,[2] Richard G. McMahon[2] and Isobel M. Hook[3]

[1]*SIRTF Science Center, California Institute of Technology, MS 100-22, Pasadena, CA 91125, USA*
[2]*Institute of Astronomy, Madingley Road, Cambridge CB3 0HA*
[3]*Institute for Astronomy, Royal Observatory, Blackford Hill, Edinburgh EH9 3HJ*

Accepted 2000 November 10. Received 2000 October 10

ABSTRACT

We present the spectra, positions, and finding charts for 31 bright ($R < 19.3$) colour-selected quasars covering the redshift range $z = 3.85$–4.78, with four having redshifts $z > 4.5$. The majority are in the southern sky ($\delta < -25°$). The quasar candidates were selected for their red ($B_J - R \gtrsim 2.5$) colours from UK or POSSII Schmidt Plates scanned at the Automated Plate Measuring (APM) facility in Cambridge. Low-resolution ($\gtrsim$10 Å) spectra were obtained to identify the quasars, primarily at the Las Campanas Observatory. The highest redshift quasar in our survey is at $z \approx 4.8$ ($R = 18.7$) and its spectrum shows a damped Lyα absorption system at $z = 4.46$. This is currently the highest redshift damped Lyα absorber detected. Five of these quasars exhibit intrinsic broad absorption line features. Combined with the previously published results from the first part of the APM United Kingdom Schmidt Telescope (UKST) survey we have now surveyed a total of $\sim$8000 deg^2 of sky i.e. 40 per cent of the high galactic latitude ($|b| > 30°$) sky, resulting in 59 optically selected quasars in the redshift range 3.85 to 4.78; 49 of which have $z \geq 4.00$.

Key words: surveys – quasars: absorption lines – quasars: emission lines.

1 INTRODUCTION

High-redshift quasars provide a powerful means for exploring early epochs. It is likely that they flag regions where galaxy formation is very active. Their host galaxies are probably still forming and they may occur in the exceptional '5σ' peaks in the matter distribution of the early Universe. In addition to being of intrinsic interest themselves, bright high-redshift quasars are particularly valuable as probes of the intervening gas clouds and galaxies superimposed on their spectra in absorption. The galaxies that intercept their line of sight provide samples selected by gas cross-section, without regard to their surface brightness, luminosity, or star formation rate. Although direct studies of high-redshift galaxies are now possible, those selected by the absorption lines they produce in quasar spectra still provide the only means to study in detail their kinematic properties at high resolution. This information can be combined with the colour and morphological information obtained from imaging to provide a complete picture of individual galaxies at high redshift.

In 1996 we published spectra for 28 quasars discovered in the first APM Colour Survey for high-redshift quasars (Storrie-Lombardi et al. 1996, hereafter APM1). These were located at equatorial declinations. We have completed the second APM Colour Survey for bright, $z > 4$ quasars in the southern hemisphere (mainly with $\delta < -25°$), discovering 23 more high-redshift quasars. We also include eight previously unpublished quasars also found using this same technique that were not directly part of the Las Campanas follow-up campaign. Three other lower redshift quasars ($z = 0.40$–2.73) were also found serendipitously in the survey and we include their spectra for completeness.

The paper is organized as follows. In Section 2 we discuss the methodology of the quasar candidate selection, in Section 3 we describe the observations and present the spectra, in Section 4 we discuss some of the objects individually, and in Section 5 we provide a summary discussion.

2 QUASAR CANDIDATE SELECTION

The quasar candidates were generally selected of the basis of their exceptionally red $B_J - R$ colour (Irwin, McMahon & Hazard 1991a), although in a few cases the addition of an I passband enabled selection closer to the main stellar locus to be made. All of the quasars bar one, BR J1603+0721, were found using B_J, R[1] and, occasionally, I passband UK Schmidt plates. In all cases these plates came from the generic southern sky survey material taken

[1] For simplicity we will use R to denote either R or OR (the majority) plates. The OR passband is the official UKST survey band and covers the wavelength range 5900–6900 Å. Earlier 'B' grade survey plates were often taken in the R passband covering 6300–6900 Å, some of which were used during the course of our survey.

★ E-mail: lisa@ipac.caltech.edu

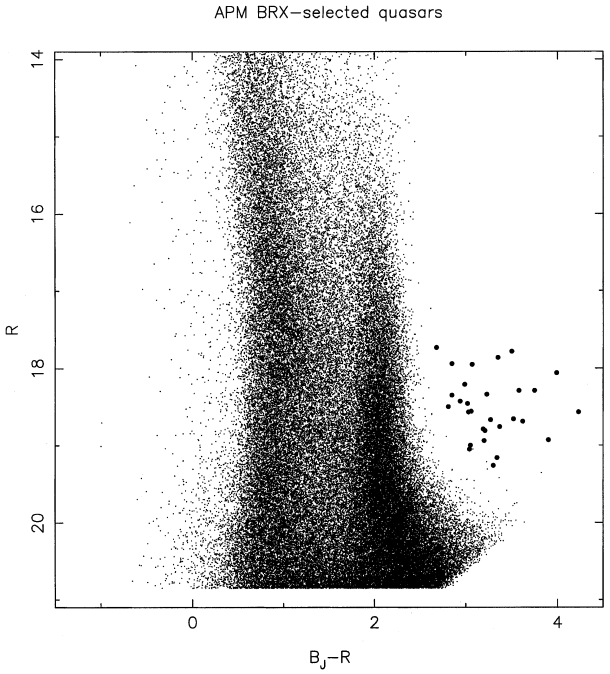

Figure 1. A B_J, R colour–magnitude diagram for a typical high-latitude UKST field used in the APM survey. Every detected B_J, R matched pair of objects classified as stellar on the R plate is plotted as small dot. Overlaid as filled circles are the complete southern sample of BRX-selected quasars.

by the UK Schmidt telescope (UKST) and were either glass copies of 'A' grade survey B_J plates, or original survey OR/R and I plates. The Northern object was found as part of a test series of measurements of POSSII survey (i.e. second epoch Palomar Sky Survey) B_J glass copies matched to POSSII R survey film copies.

All plate material was measured and analysed at the Automated Plate Measuring (APM) facility in Cambridge, UK, to produce image lists including classification, magnitude and colour information (for further details see Kibblewhite et al. 1984; Irwin, Demers & Kunkel 1990). A large fraction of the UKST survey plates were measured over a 5-yr period from 1989. Consequently, many of the final survey grade UKST plates were not available at scanning time and in several cases early 'B' grade survey plates were used instead.

At an early stage in the programme we decided to restrict the candidate selection to those stellar objects lying well away from the main stellar locus and to relatively bright magnitudes. This was mainly to increase the efficiency of the spectroscopic follow-up and also because the primary goal of the programme was to find a bright sample of quasars for further absorption line follow-up studies. In addition, the multi-epoch nature of the plate material precludes attaining completeness based solely on colour/magnitude information owing to the intrinsic variability of quasars (see for example Hook et al. 1994 and references therein). The effects of colour selection on sample completeness have been thoroughly investigated over the past few years (e.g. Warren, Hewett & Osmer 1994; APM1; Kennefick, Djorgovski & de Carvalho 1995 and references therein).

The efficacy of the traditional two-colour selection for finding $z > 4$ quasars based on B_J, R, I photometry is shown in fig. 1 of Irwin et al. (1991a). Since most of the current sample of quasars were selected using what we have called the 'BRX' technique, we demonstrate this method in the current paper. Fig. 1 shows a B_J, R colour–magnitude diagram for a typical high-latitude UKST field. Every detected B_J, R matched pair of objects classified as stellar on the R plate is plotted as a small dot. Overlaid as filled circles are the complete southern sample of BRX-selected quasars. Of the roughly 250 000 paired objects on each high-latitude UKST field, two-thirds are classified as stellar on the R plate and roughly 50 000 of these are brighter than $R = 19$–19.5, the range for the R-magnitude limit. Although the aim was to find bright $R \lesssim 19$-mag quasars, rather than impose a rigid magnitude cut we allowed the faint limit to reach 19.5 if the plate pairs were of suitably good quality and had a clean colour–magnitude diagram at this limit.

The red boundary for BR candidate selection was set to approximately $B_J - R = 2.5$ for images brighter than $R = 18.5$ and was then increased roughly linearly to $B_J - R = 3$ at $R = 19.5$. This results in a very clean sample, as can be seen from Fig. 1, with usually at most 10 candidates per field. Roughly half of the candidates can be easily rejected using the online APM catalogue finding charts. These rejected objects would typically be objects: close to the edge of the scanned area on one or other plate; in, or near, the halo of bright stars; affected by some scratch or satellite trail; close to one of the density wedges; and so on.

A schematic representation of the area of sky surveyed in the current work, together with those areas surveyed in our previously published sample (APM1), is given in Fig. 2. The total area of Southern high-latitude sky surveyed is roughly 8000 deg^2 from a total of 328 UKST fields. Although the measured area of each field amounts to some 5.8×5.8 deg^2, the effective area of each field is only $\approx$25 deg^2. This is mainly as a result of the 5° grid spacing of the survey but also involves reductions because of the effect of density wedges and general edge effects. The majority of the fields used are high latitude in the sense that $|b| > 30°$, however there are a small number of fields closer to the Galactic Plane than that, since the survey data were measured for a variety of projects.

External deep photometric calibration did not (and still does not) exist for the majority of the fields surveyed. However, as in earlier work using the APM facility, we used an internal plate calibration method (Bunclark & Irwin 1983) as the basis of a (mainly) internal calibration scheme. Making use of the uniformity in depth of the Schmidt survey plates and the fact that colour equations for UKST plate/filter combinations are well known (e.g. Blair & Gilmore 1982; Irwin, Demers & Kunkel 1990) facilitates use of a natural photographic passband magnitude scale. Although from external sequence checks the faint stellar R-band magnitude scale can only be tied down to an rms variation of 0.25 mag with this method, the known properties of Galactic foreground stars can be readily used to define the $B_J - R$ colour to an accuracy of 0.1 mag. This, and a reliable star–galaxy classifier, make candidate selection extremely straightforward.

3 OBSERVATIONS

Candidate follow-up proceeded over several years, using a range of facilities (see Table 1 column 10), with the majority of the follow-up taking place at Las Campanas during three spectroscopic runs in 1997 and 1998. Candidates were generally prioritized for observation on the extremity of their $B_J - R$ colour and on their relative brightness. Although we have not observed more than $\approx$50 per cent of the total number of candidates, spectra have been obtained for all of the most promising objects. In several fields where early on during the survey we observed all the

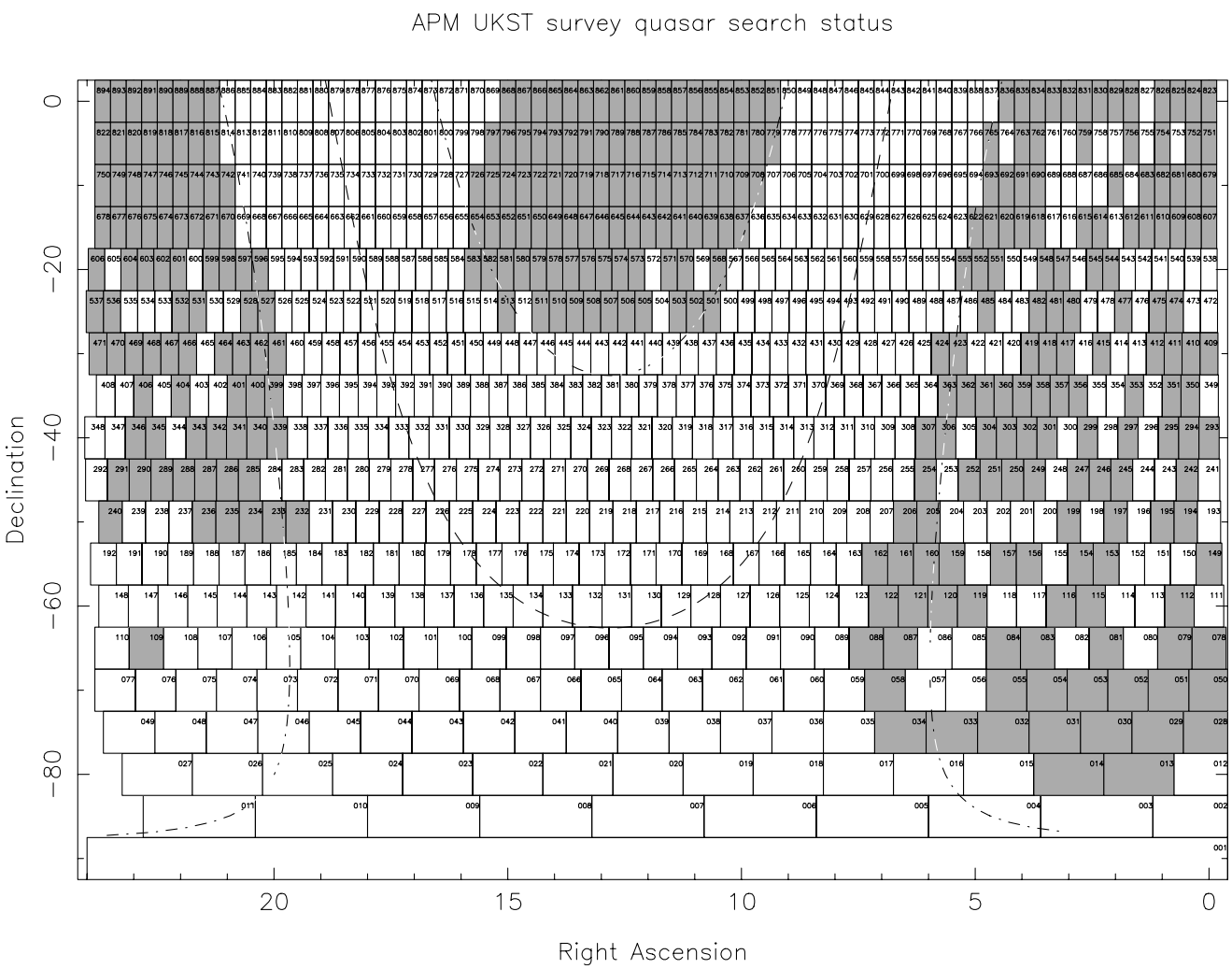

Figure 2. Plotted here is a schematic representation of the area of sky surveyed in the current work, together with those areas surveyed in our previously published sample (Storrie-Lombardi et al. 1996). The total area of Southern high-latitude sky surveyed is roughly 8000 deg^2 from a total of 328 UKST fields. The dot–dash lines denote the $|b| = 30°$ Galactic latitude locii.

candidates, we found that objects near the stellar locus invariably turned out to be late M-type stars shifted out of the main locus by the inevitable non-Gaussian tale of the photometric errors. In subsequent observing runs we were more conservative in candidate selection in order to speed up the progress of the survey.

For the follow-up undertaken at the Dupont 100-inch telescope at Las Campanas we used the Modular Spectrograph with the 300 line mm^{-1} grating and the Tek#5 CCD, in gray and bright time. This gives wavelength coverage from approximately 4000–9000 Å (2.5 Å pixel^{-1}) which easily covers the Lyα and C IV emission lines and the Lyα forest drop for quasars with $4 < z < 5$. Typical exposure times were 600–900 s which allowed differentiation between high-redshift quasars with a continuum drop across the Lyα line caused by intervening cosmological absorption, and M-dwarfs or galaxies at $z \sim 0.3$, the main contaminants in the survey. The spectra were reduced as they were taken using standard IRAF[2] routines which allowed us to follow-up in real time any candidates where the first spectrum did not make it immediately clear whether it was a quasar or not. For every 8–10 candidates remaining from the selection in Section 2, one is a high-redshift quasar. The additional observations were also taken at low resolution on a variety of facilities during other observing runs between 1986–1997, mainly at times when the primary observing programme could not be executed.

Throughout the survey, apart from high-redshift quasars, the only 'real' objects we have found lying significantly redward of the K/M stellar locus are: misclassified compact galaxies, usually ellipticals at redshift 0.3–0.4, where the 4000-Å break has left the B_J passband at 5400 Å; very late-type M giants including Miras and other long period variables; distant halo carbon stars (e.g. Totten & Irwin 1998); very late-type – often high proper motion – nearby dwarf M stars (Irwin et al. 1991b; Kirkpatrick, Todd & Irwin 1997) and at least one field brown dwarf (Tinney 1998); and the occasional Cepheid variable and/or planetary nebulae.

The quasars discovered are listed in Table 1. The quasars were originally selected off photographic plates using B1950 coordinates as the default equinox, but we have listed their names with the J2000 coordinate system as well for ease of cross-reference.

[2] IRAF is distributed by the National Optical Astronomy Observatories, which is operated by the Association of Universities for Research in Astronomy, Inc. (AURA) under cooperative agreement with the National Science Foundation.

Table 1. Second APM Colour Survey quasars – journal of observations.

Quasar Name	RA (B1950)	Dec. (B1950)	Quasar Name	RA (J2000)	Dec. (J2000)	R	$B_J - R$	Plate ID	Telescope/Date Observed	Exp. Secs	Redshift
†BR B0002−6712	00 02 04.22	−67 12 08.6	BR J0004−6655	00 04 35.67	−66 55 26.4	17.78	2.97	F078	LCO/1997 Oct 18	600	2.73
BR B0004−6224	00 04 20.98	−62 24 45.7	BR J0006−6208	00 06 51.61	−62 08 03.7	18.29	3.58	F078	LCO/1997 Oct 22	1300	4.51
†BR B0016−3544	00 16 07.77	−35 44 19.7	BR J0018−3527	00 18 37.87	−35 27 40.3	18.43	2.94	F350	LCO/1998 Nov 1,5	1500	4.15
BR B0028−5146	00 28 11.42	−51 46 20.4	BR J0030−5129	00 30 34.37	−51 29 46.3	18.57	3.03	F194	LCO/1997 Oct 18	700	4.17
†BR B0044−1622	00 44 15.55	−16 22 44.5	BR J0046−1606	00 46 45.44	−16 06 21.8	18.21	2.99	F609	WHT/1995 Aug 31	600	3.85
BRI B0046−2458	00 46 07.18	−24 58 27.1	BRI J0048−2442	00 48 34.57	−24 42 06.0	18.94	2.32	F474	AAT/1989 Sep 7	1200	4.15
BRI B0111−2819	01 11 21.80	−28 19 09.8	BRI J0113−2803	01 13 44.37	−28 03 17.2	18.67	3.27	F412	AAT/1989 Sep 6	1600	4.30
BRI B0135−4239	01 35 15.70	−42 39 31.9	BRI J0137−4224	01 37 24.41	−42 24 16.8	18.46	1.88	F297	CTIO/1986 Sep 4	450	3.97
BR B0232−1819	02 32 35.08	−18 19 13.6	BR J0234−1806	02 34 55.14	−18 06 08.5	18.79	3.19	F545	LCO/1998 Nov 2	600	4.30
BR B0259−5548	02 59 57.35	−55 48 58.3	BR J0301−5537	03 01 21.55	−55 37 11.6	19.00	3.05	F154	LCO/1997 Oct 21	600	4.11
†BR B0300−0207	03 00 21.00	−02 07 50.4	BR J0302−0156	03 02 53.06	−01 56 05.7	18.56	3.06	F832	WHT/1995 Aug 31	600	4.25
BR B0305−4957	03 05 46.75	−49 57 16.1	BR J0307−4945	03 07 22.88	−49 45 48.0	18.76	3.37	F199	LCO/1997 Oct 22	900	4.78
BR B0308−1734	03 08 56.99	−17 34 04.3	BR J0311−1722	03 11 15.20	−17 22 47.4	17.73	2.68	F547	LCO/1998 Nov 7	600	4.00
BR B0322−2928	03 22 39.77	−29 28 52.9	BR J0324−2918	03 24 44.28	−29 18 21.1	18.66	3.52	F418	LCO/1998 Nov 2	600	4.62
BR B0331−1622	03 31 55.37	−16 22 04.7	BR J0334−1612	03 34 13.45	−16 12 05.2	17.86	3.35	F618	WHT/1995 Aug 31	600	4.32
BR B0353−3820	03 53 16.10	−38 20 25.4	BR J0355−3811	03 55 04.87	−38 11 42.3	17.95	3.07	F302	LCO/1997 Oct 18	500	4.58
BR B0413−4405	04 13 39.30	−44 05 18.4	BR J0415−4357	04 15 15.17	−43 57 52.9	18.81	3.21	F250	LCO/1997 Oct 20	600	4.08
BR B0418−5723	04 18 51.49	−57 23 19.6	BR J0419−5716	04 19 50.94	−57 16 13.0	17.78	3.50	F157	LCO/1997 Oct 20	400	4.37
BR B0424−2209	04 24 01.44	−22 09 00.6	BR J0426−2202	04 26 10.33	−22 02 17.3	17.94	2.85	F551	LCO/1998 Nov 5	600	4.30
BR B0523−3345	05 23 16.53	−33 45 41.5	PMN J0525−3343	05 25 06.17	−33 43 05.5	18.50	2.81	F363	LCO/1997 Oct 22	600	4.40
BR B0527−3528	05 27 29.28	−35 28 21.6	BR J0529−3526	05 29 15.89	−35 26 03.6	18.94	3.20	F363	LCO/1997 Oct 22	700	4.41
BR B0527−3554	05 27 34.98	−35 54 51.7	BR J0529−3552	05 29 20.81	−35 52 34.1	18.29	3.75	F363	LCO/1997 Oct 22	400	4.15
BR B0714−6449	07 14 12.70	−64 49 51.2	BR J0714−6455	07 14 31.37	−64 55 10.6	18.35	2.85	F088	LCO/1997 Oct 22	1200	4.47
BR B1307−1724	13 07 46.61	−17 24 31.7	BR J1310−1740	13 10 26.62	−17 40 28.5	19.26	>3.30	F646	WHT/1997 Apr 29	300	4.20
BR B1328−2506	13 28 06.26	−25 06 52.1	BR J1330−2522	13 30 51.98	−25 22 18.8	18.46	3.02	F509	LCO/1997 Apr 13	600	3.91
BR B1444−2104	14 44 09.82	−21 04 31.3	BR J1447−2117	14 47 00.66	−21 17 03.1	18.84	3.06	F580	LCO/1997 Apr 13	600	0.40
BR B1600+0729	16 00 54.77	+07 29 17.5	BR J1603+0721	16 03 20.91	+07 21 04.6	18.93	3.90	F799	KPNO/1995 May 24	500	4.35
BR B2012−4041	20 12 00.09	−40 41 41.2	BR J2015−4032	20 15 21.65	−40 32 29.0	18.58	2.85	F340	LCO/1997 Oct 20	400	0.68
†BR B2013−4028	20 13 56.20	−40 28 43.1	BR J2017−4019	20 17 17.12	−40 19 24.0	18.57	4.23	F340	LCO/1997 Oct 20	400	4.15
†BR B2128−4442	21 28 25.67	−44 42 32.6	BR J2131−4429	21 31 39.50	−44 29 17.2	18.34	3.23	F287	LCO/1997 Oct 20	400	3.83
BR B2213−6729	22 13 07.32	−67 29 43.1	BR J2216−6714	22 16 51.98	−67 14 43.5	18.06	3.99	F109	LCO/1998 Nov 2	1500	4.49
BR B2314−4401	23 14 40.86	−44 01 51.5	BR J2317−4345	23 17 26.84	−43 45 27.5	19.05	3.04	F291	LCO/1997 Oct 22	900	4.02
BR B2326−4530	23 26 05.30	−45 30 17.8	BR J2328−4513	23 28 48.60	−45 13 45.6	19.16	3.34	F291	LCO/1997 Oct 18	800	4.38
BR B2346−3729	23 46 37.36	−37 29 39.8	BR J2349−3712	23 49 13.76	−37 12 58.9	18.69	3.62	F293	LCO/1998 Nov 3	600	4.21

† These quasars exhibit intrinsic broad absorption line (BAL) characteristics.

Note: The quasars with prefix BR were selected by the $B_J - R$ excess method and those with the prefix BRI were selected using the two-colour method. The quasar with prefix PMN was selected using the $B_J - R$ excess method and radio data.

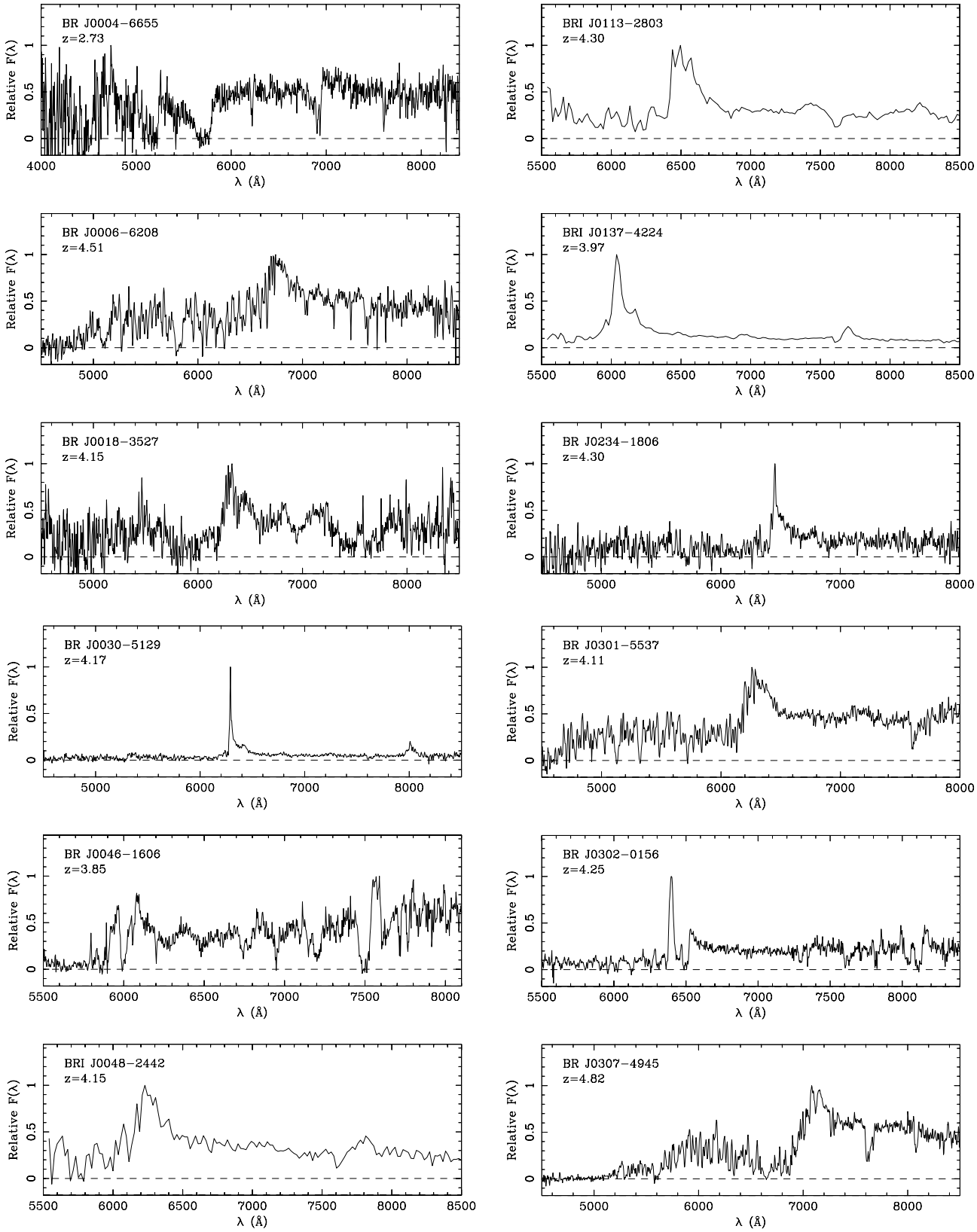

Figure 3. The quasar discovery spectra are shown.

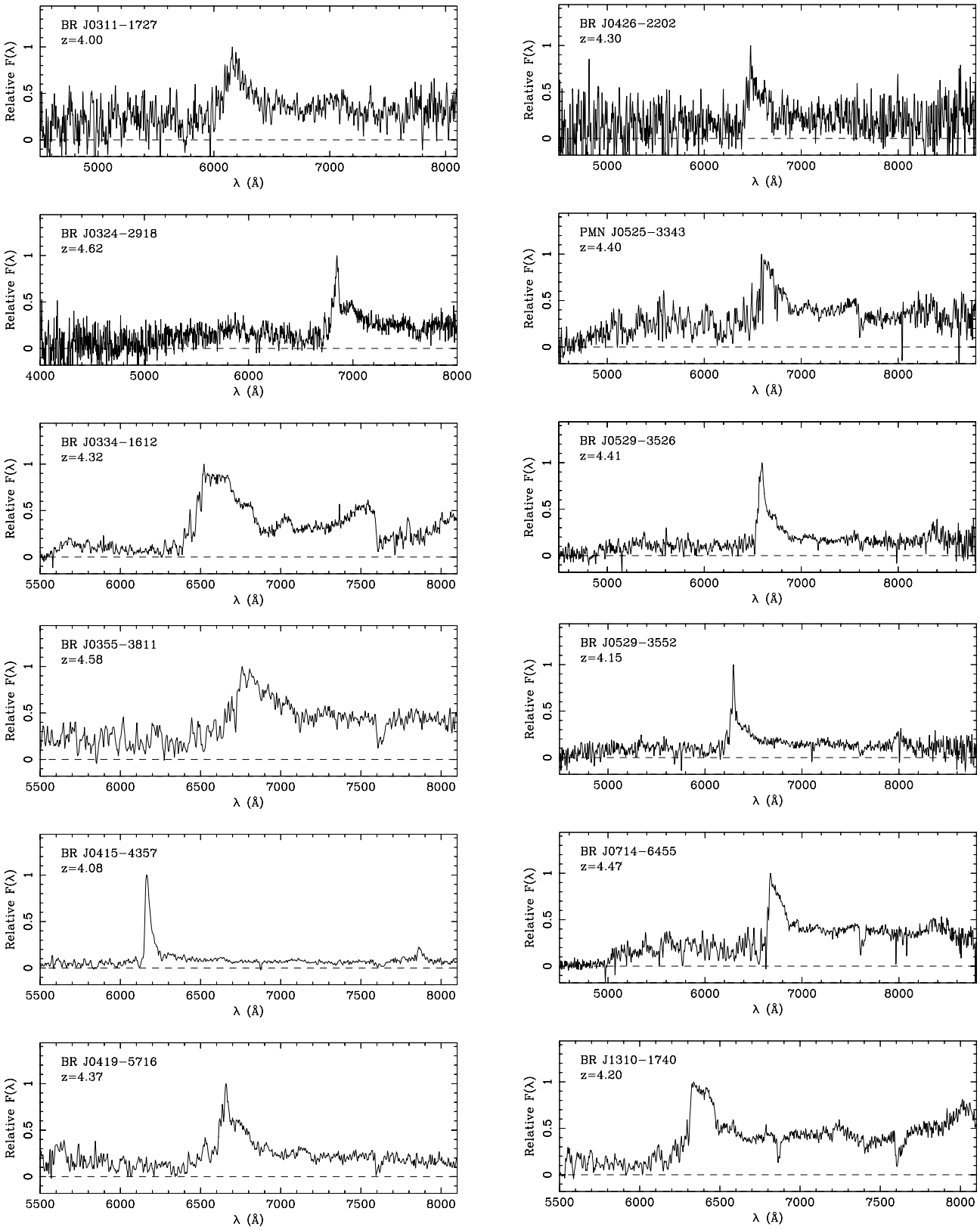

Figure 3 – *continued*

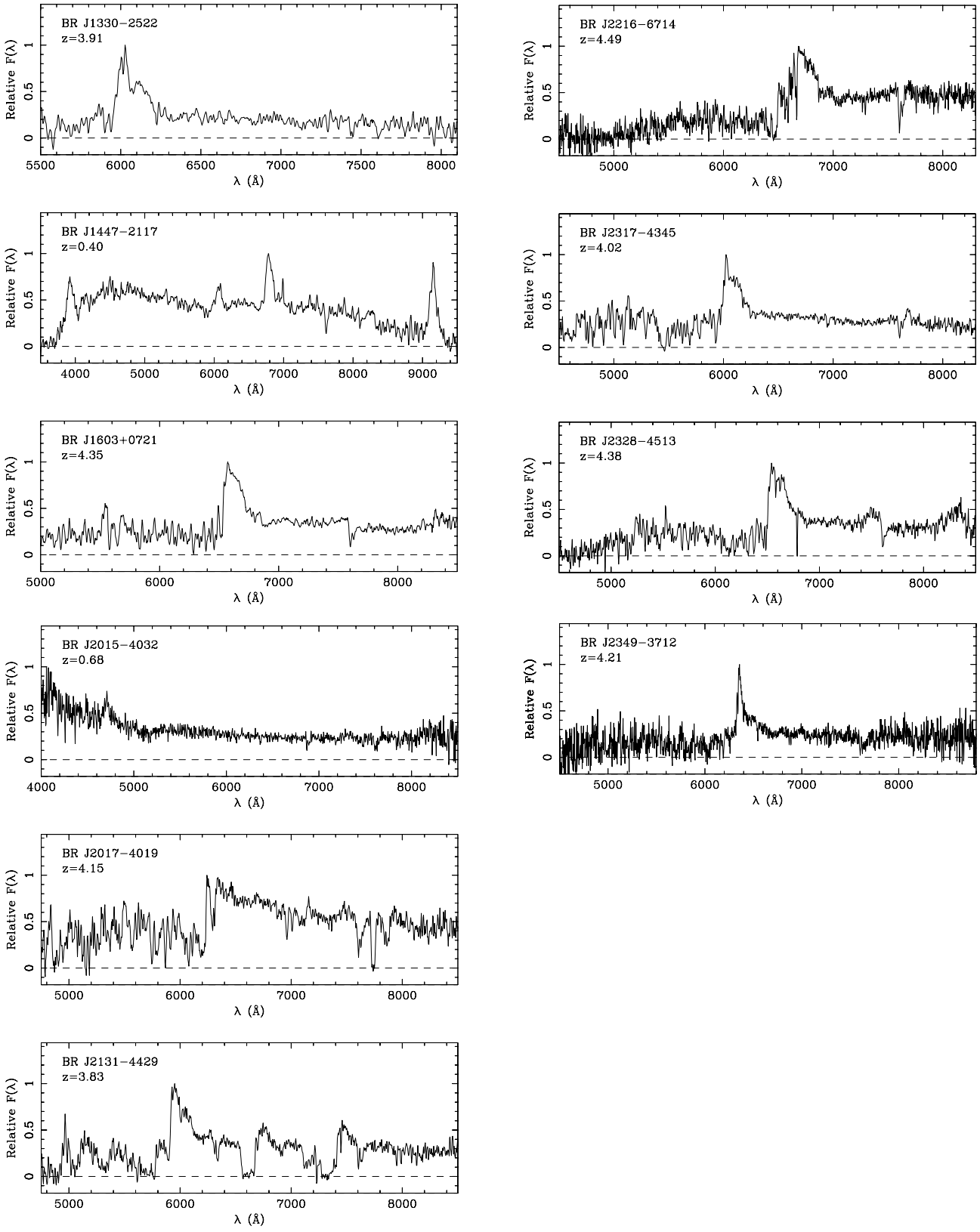

Figure 3 – *continued*

Columns 1, 2 and 3 list the quasar name, right ascension and declination in B1950 coordinates and columns 4, 5 and 6 give the same information in the J2000 equinox. Columns 7, 8 and 9 list the APM R magnitude, the APM $B_J - R$ colour, and the plate number off which the object information was measured. Column 10 lists where and when the observations were made. The abbreviations are: LCO = Dupont 100-inch – Las Campanas Observatory, AAT = 4.3 – m Anglo-Australian Telescope,

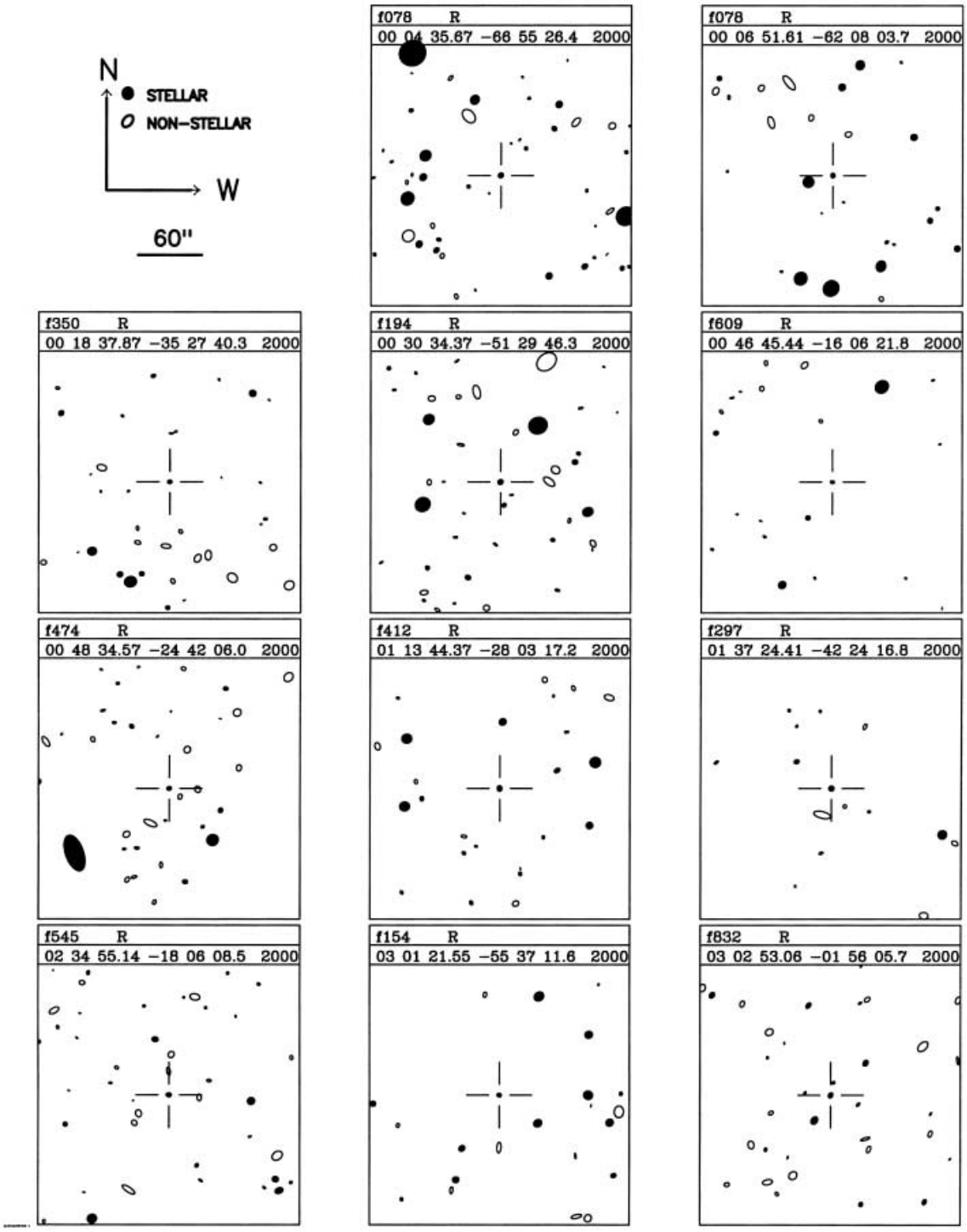

Figure 4. The finding charts for the Second APM Colour Survey quasars are shown. Each is 5 arcmin on a side, oriented with north up and west to the right.

WHT = 4.2 − m William Herschel Telescope, CTIO = Blanco 4-m – Cerro Tololo Inter-American Observatory, and KPNO = Mayall 4-m – Kitt Peak National Observatory. Column 11 gives the total exposure time for each spectrum, and column 12 the quasar redshifts determined from these spectra. The redshifts were generally determined from the blueward edge of the Lyα emission unless the spectrum had a high enough signal-to-noise ratio to measure the C IV emission line. Previous experience has shown that the uncertainties in the redshifts measured from these discovery spectra will be ± 0.1. Five of the quasars exhibit intrinsic broad absorption line (BAL) features. These are noted in the table. The spectra are shown in Fig. 3 and the finding charts in Fig. 4. The O_2 A-band absorption feature at 7600 Å has not been removed from any of the spectra. In addition to the 31 high-redshift quasars we also list three additional lower redshift objects discovered as part of our Las Campanas survey. These include a broad absorption line quasar at $z = 2.73$ and quasars at redshifts $z = 0.40$ and 0.68.

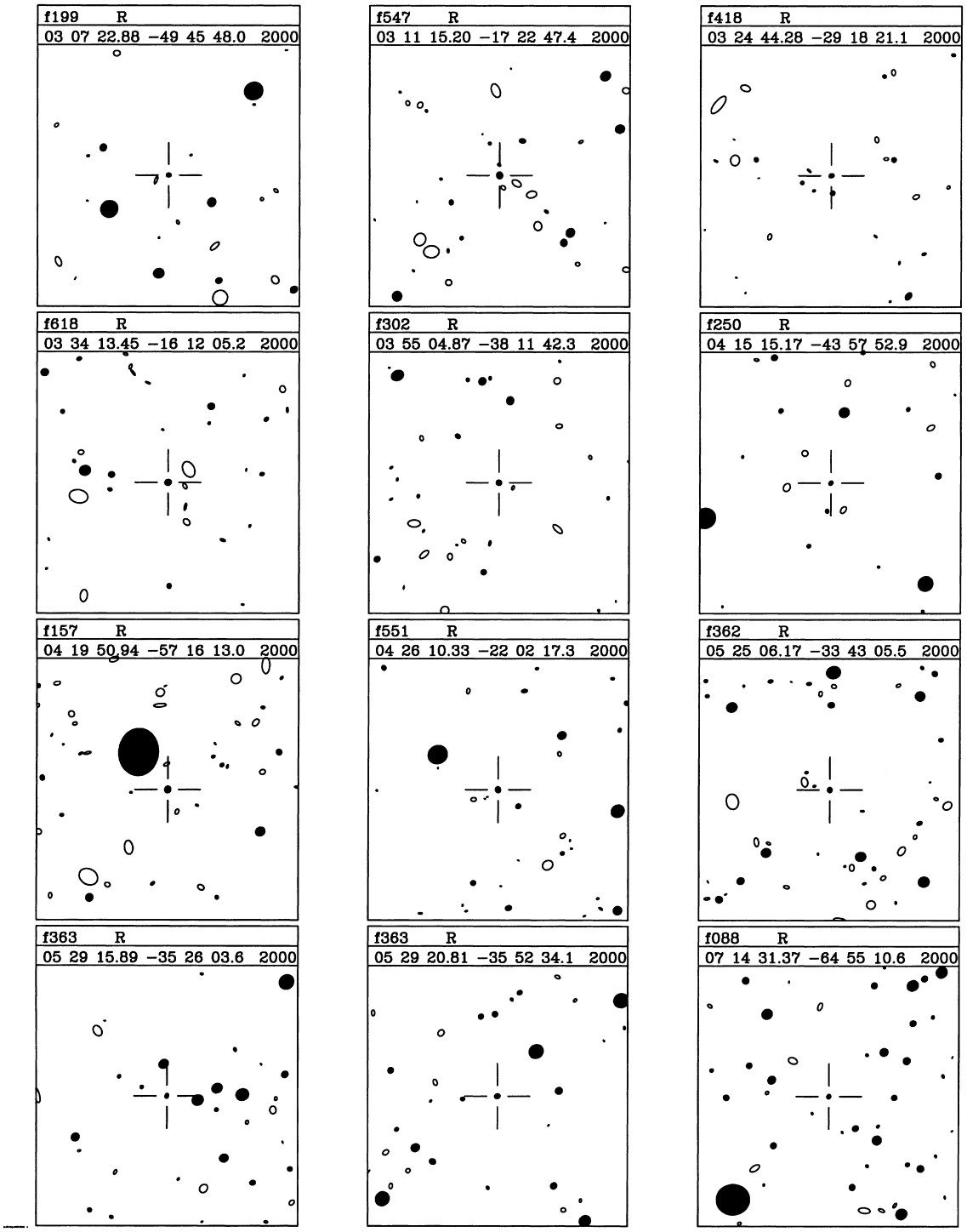

Figure 4 – *continued*

4 NOTES ON INDIVIDUAL OBJECTS

Higher resolution spectroscopy of these quasars is necessary to do quantitative studies of their emission and absorption line properties (see Péroux et al. 2001) but many interesting features are apparent in the discovery spectra.

(1) BR J0004−6655, $z = 2.73$ BAL

This quasar exhibits broad absorption lines. It is intrinsically red in the optical $B_J - R$ colours owing to the broad absorption line troughs redward of 5900 Å.

(2) BR J0006−6208, $z = 4.51$

This spectrum shows evidence for two damped Lyα absorption candidates at $z \approx 3.2$ and $z \approx 3.8$ and a Lyman limit system at $z \approx 3.2$. The Lyα emission line is relatively weak, but not atypical of $z > 4$ quasars.

(3) BR J0018−3527, $z = 4.15$ BAL

This quasar exhibits broad absorption line features.

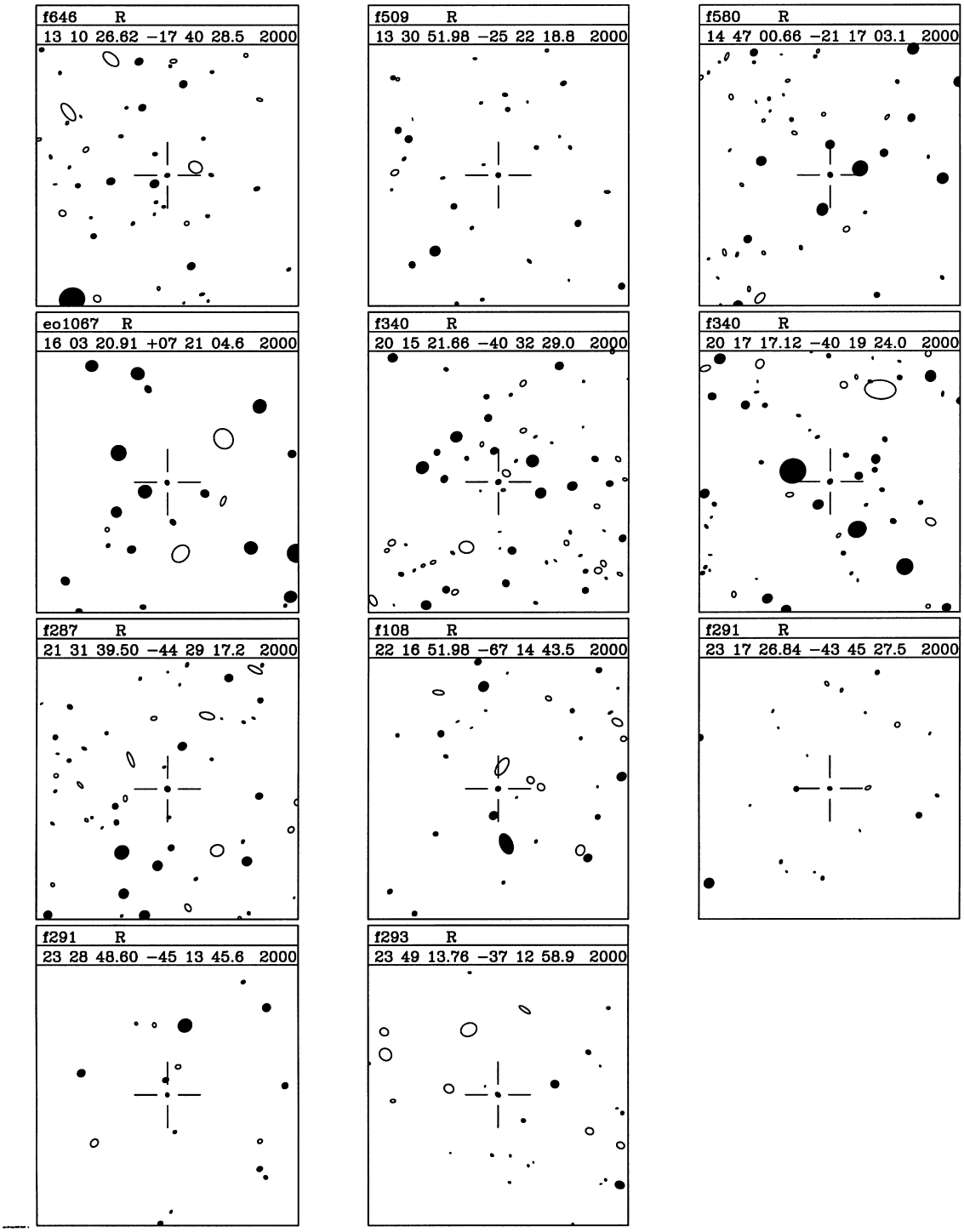

Figure 4 – *continued*

(4) BR J0030−5129, $z = 4.17$

This quasar shows very strong, peaky emission lines and in conjunction with the previous two objects demonstrates the wide variety of quasar spectra found in photographic multicolour surveys.

(5) BR J0046−1606, $z = 3.85$*BAL*

This quasar exhibits broad absorption line features which enhance the red optical colour at this relatively low redshift.

(6) BRI J0048−2442, $z = 4.15$

(7) BRI J0113−2803, $z = 4.30$

(8) BRI J0137 − 4224, $z = 3.97$

Nothing much is evident in these three ≈50-Å resolution spectra taken in the late 1980s, other than the fact that these objects are quasars. Higher resolution spectra have been taken of these quasars in a recent survey for absorption lines systems (Storrie-Lombardi & Wolfe 2000). BRI J0137−4224 is of interest since it was the first APM BRI-selected quasar to be found, thereby proving the concept, and was discovered at CTIO in 1986 shortly after the first redshift 4 quasar was found by Warren et al. (1987).

(9) BR J0234−1806, $z = 4.30$

This quasar has strong Lyα emission. The apparently negative flux regions around 4000–5000 Å are due to a combination of poor signal-to-noise ratio and imperfect sky subtraction.

(10) BR J0301−5537, $z = 4.11$

A well-defined Lyman limit system is apparent at $z \approx 4.0$.

(11) BR J0302−0156, $z = 4.25$ BAL

This quasar shows broad absorption line features.

(12) BR J0307−4945, $z = 4.78$

This is the highest redshift quasar in our survey. It shows a damped Lyα absorption feature at $z = 4.46$. Both the Lyα and Lyβ lines are visible at 6650 and 5605 Å. This absorption system is discussed in more detail in McMahon et al. (in preparation), Péroux et al. 2001, and Dessauges-Zavadsky et al. (2001). It is currently the highest redshift damped absorber known.

(13) BR J0311−1727, $z = 4.00$

A candidate damped Lyα absorber is detected at $z \approx 3.7$.

(14) BR J0324−2918, $z = 4.62$

This is the second highest redshift quasar in the current sample.

(15) BR J0334−1612, $z = 4.32$

A higher resolution spectrum of this quasar is shown in Storrie-Lombardi & Wolfe (2000).

(16) BR J0355−3811, $z = 4.58$

An strong Mg II absorption feature is evident at $z = 1.99$.

(17) BR J0415−4357, $z = 4.08$

This is another quasar with a very strong Lyα emission line.

(18) BR J0419−5716, $z = 4.37$

No comments.

(19) BR J0426−2202, $z = 4.30$

This is a very poor signal-to-noise ratio but not atypical discovery spectrum, confirmed by later better quality spectroscopy.

(20) PMN J0525−3343, $z = 4.40$

This quasar was detected using the BRX technique and also independently discovered as a radio-loud quasar by Hook et al. (in preparation). The spectrum is unusual for high-redshift radio-loud quasars as the Lyα line is much weaker than normally found.

(21) BR J0529−3526, $z = 4.41$

(22) BR J0529−3552, $z = 4.15$

No comments.

(23) BR J0714−6455, $z = 4.47$

This quasar shows a Lyman limit system (and possible damped Lyα candidate) at $z \approx 4.4$.

(24) BR J1310−1740, $z = 4.20$

(25) BR J1330−2522, $z = 3.91$

No comments.

(26) BR J1447−2117, $z = 0.40$

This low-redshift quasar is relatively blue in $B_J - R$ and must have entered the sample through intrinsic variability. The epoch difference between the plate pairs was large (18 yr).

(27) BR J1603+0721, $z = 4.35$

A higher resolution spectrum of quasar this quasar is shown in Storrie-Lombardi & Wolfe (2000). This object is notable because it was discovered using the POSSII glass and film copies.

(28) BR J2015−4032, $z = 0.68$

This low-redshift quasar is relatively blue in $B_J - R$ and must have entered the sample through intrinsic variability. The epoch difference between the plate pairs was large (15 yr).

(29) BR J2017−4019, $z = 4.15$ BAL

The Lyα and C IV emission lines in this quasar are almost completely absorbed giving the spectrum the appearance of a step-function.

(30) BR J2131−4429, $z = 3.83$ BAL

This quasar shows classic broad absorption line features.

(31) BR J2216−6714, $z = 4.49$

There is a possible double damped Lyα absorber at z ≈ 4.3.

(32) BR J2317−4345, $z = 4.02$

There is a damped Lyα candidate at $z = 3.4$.

(33) BR J2328−4513, $z = 4.38$

(34) BR J2349−3712, $z = 4.21$

No comments.

5 DISCUSSION

The only other comparable bright large-area high-redshift survey is that of Kennefick et al. (1995 and references therein, see also http://astro.caltech.edu/~george/z4.qsos). Although this survey is based on POSSII photographic *B*, *R* and *I* plates, the underlying methodology is essentially the same as that described in Irwin et al. (1991a). In the first phase of this survey 10 quasars at redshifts >4 were found, selected from 27 fields covering an area of 681 deg^2.

Combining the results from the First APM Colour Survey for High Redshift Quasars (APM1) with the work presented in this paper we have found a total of 59 bright high-redshift quasars ($R \leq 19.5$; $3.8 < z < 4.8$) in a survey of approximately 8000 deg^2 of the southern and equatorial sky. In Fig. 5 we show two histograms of the redshift distribution of the combined APM Colour Surveys. The left panel shows the combined histogram with the BR-selected quasars shown with single hatch marks and the BRI-selected quasars shown with the double hatch marks. The right-hand panel again shows the combined survey histogram, with hatch marks overlaid on the quasars that exhibit broad absorption lines (BAL) characteristics.

The histograms highlight several important characteristics of the BR(I) survey.

(i) There is a well-defined upper redshift limit to which the survey is sensitive. This upper limit is primarily caused by the *R*-band emulsion cut-off at 6900 Å and represents the point where the redshifted Lyα line moves out of the *R*-band. Consequently the entire *R*-band flux lies within the Lyα forest and the intrinsic strong 'continuum drop' across Lyα causes the *R*-band magnitude selection boundary to move to even brighter absolute magnitudes on the quasar luminosity function, with a corresponding dramatic fall in the expected number of quasars. The other compounding factor at $z > 5$ is the statistical proximity of Lyman limit systems to the redshift of the quasar (e.g. Storrie-Lombardi et al. 1994). This means that even bright quasars are not detected on the B_J plates, which have a limit of roughly $B_J = 22.5$.

(ii) The roll-over in numbers at redshift $z = 4.2$ is mainly caused by the candidate selection for the majority of the fields making use of the BR selection technique. Although, we are dealing with small number statistics, it is clear that the BRI technique can be used to somewhat lower redshifts, $z = 4.0$, in general. This is simply because the extra leverage obtained from the *I*-band enables candidates to be selected closer to the stellar locus. For example, it is clear from comparing fig. 1 of Irwin et al. (1991a), with Fig. 1 in the current paper, that BR-selected candidates are a subset of BRI-selected objects.

(iii) In general the BAL quasars appear to be at redshifts significantly lower than 'normal' quasars. This is also a selection bias owing to the fact that in addition to the usual strong absorption troughs blueward of the standard quasar emission lines,

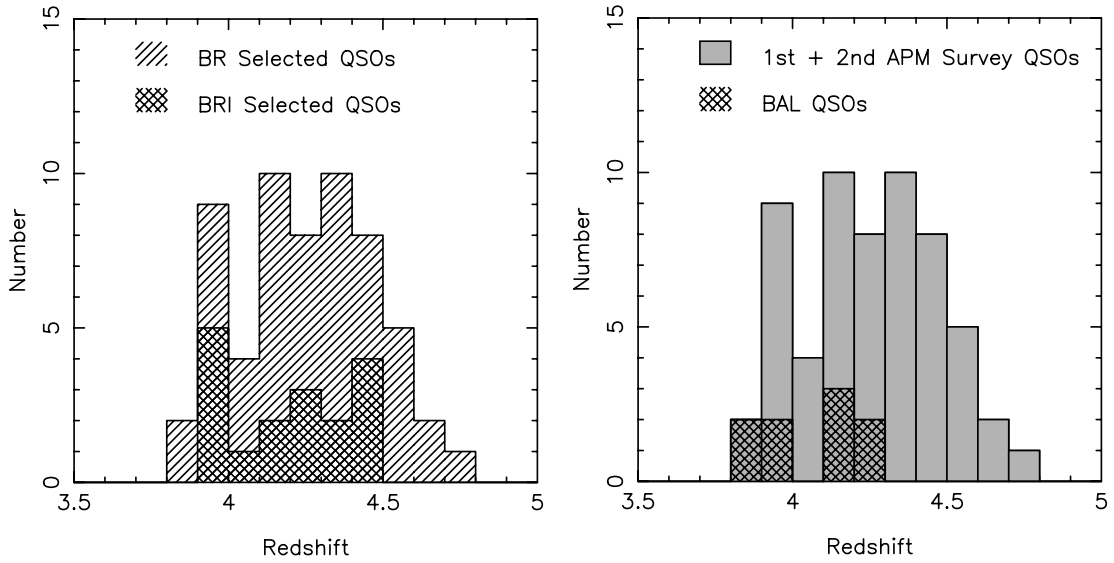

Figure 5. These histograms show the combined redshift distribution for the quasars discovered in the First and Second APM Colour Surveys for $z > 4$ quasars (Storrie-Lombardi et al. 1996; this paper). The left panel shows the complete histogram with the BR-selected quasars shown with single hatch marks and the BRI-selected quasars shown with the double hatch marks. The right panel again shows the combined survey histogram fully shaded, with hatch marks overlaid on the quasars that exhibit broad absorption lines (BAL) characteristics.

BAL quasars have strong Lyman limit systems at the redshift of the quasar. This depresses the B_J band flux more than for normal quasars enabling them to be selected just below redshift $z = 4$ and also causes the flux to be depressed to such a low level that they no longer register on the B_J plates at redshifts much beyond $z = 4.3$. Indeed the highest redshift quasar without a measurable B_J flux is a BAL quasar. However, for most of the sample, we did not pursue candidates not detected on the B_J plate.

ACKNOWLEDGMENTS

We thank the support staff at the Las Campanas, Cerro Tololo, Anglo-Australian, Kitt Peak, and Royal Greenwich Observatories for their assistance in obtaining these observations. We thank the UKSTU for providing the plate material and thank the members of the APM facility, past and present, for maintaining such an excellent system.

REFERENCES

Blair M., Gilmore G., 1982, PASP, 94, 742
Bunclark P. S., Irwin M. J., 1983, Proc. Statistical Methods in Astronomy, ESA SP-201
Dessauges-Zavadsky M., D'Odorico S., McMahon R. G., Molaro P., Ledoux C., Péroux C., Storrie-Lombardi L. J., 2001, A&A, in press
Hook I. M., McMahon R. G., Boyle B. J., Irwin M. J., 1994, MNRAS, 268, 305
Irwin M. J., Demers S., Kunkel W. E., 1990, AJ, 99, 191
Irwin M. J., McMahon R. G., Hazard C., 1991, in Crampton D., eds, ASP Conf. Ser. Vol. 21, The Space Distribution of Quasars. Astron. Soc. Pac., San Francisco, p. 117
Irwin M. J., McMahon R. G., Reid N., 1991b, MNRAS, 252, 61P
Kennefick J. D., Djorgovski S. G., de Carvalho R. R., 1995, AJ, 110, 2553
Kibblewhite E. J., Bridgeland M. T., Bunclark P. S., Irwin M. J., 1984, Proc. Astronomical Microdensitometry Conference, NASA-2317
Kirkpatrick J. D., Todd H. J., Irwin M. J., 1997, AJ, 113, 1421
Péroux C., Storrie-Lombardi L. J., McMahon R. G., Irwin M. J., Hook I. M., 2001, AJ, in press
Storrie-Lombardi L. J., Wolfe A. M., 2000, ApJ, 543, 552
Storrie-Lombardi L. J., McMahon R. G., Irwin M. J., Hazard C., 1994, ApJ, 427, L13
Storrie-Lombardi L. J., McMahon R. G., Irwin M. J., Hazard C., 1996, ApJ, 468, 128 (APM1)
Totten E. J., Irwin M. J., 1998, MNRAS, 294, 1
Tinney C. G., 1998, MNRAS, 296, L42
Warren S. J. et al., 1987, Nat, 325, 131
Warren S. J., Hewett P. S., Osmer P. S., 1994, ApJ, 421, 412

This paper has been typeset from a TEX/LATEX file prepared by the author.